



**HAL**  
open science

## **MRI assessment of deformation and water loss during meat heating**

Mustapha Bouhrara, Jean-Louis Damez, Sylvie Clerjon, Abdlatif Benmoussa,  
Stéphane S. Portanguen, Cyril Chevarin, Alain Kondjoyan, J.-M. Bonny

► **To cite this version:**

Mustapha Bouhrara, Jean-Louis Damez, Sylvie Clerjon, Abdlatif Benmoussa, Stéphane S. Portanguen, et al.. MRI assessment of deformation and water loss during meat heating. 55. International Congress of Meat Science and Technology (ICoMST), Aug 2009, Copenhagen, Denmark. Meat Science, 2009, 55èmes International Congress of Meat Science and Technology (ICoMST). hal-02752497

**HAL Id: hal-02752497**

**<https://hal.inrae.fr/hal-02752497>**

Submitted on 3 Jun 2020

**HAL** is a multi-disciplinary open access archive for the deposit and dissemination of scientific research documents, whether they are published or not. The documents may come from teaching and research institutions in France or abroad, or from public or private research centers.

L'archive ouverte pluridisciplinaire **HAL**, est destinée au dépôt et à la diffusion de documents scientifiques de niveau recherche, publiés ou non, émanant des établissements d'enseignement et de recherche français ou étrangers, des laboratoires publics ou privés.

# MRI assessment of deformation and water loss during meat heating

M. Bouhrara, J.L Damez, S. Clerjon, A. Benmoussa, S. Portanguen, C. Chevarin, A. Kondjoyan and J.M Bonny.

**Abstract** — The understanding and control of structural and physical changes in meat during cooking is essential for both meat industries and consumers. Magnetic resonance imaging (MRI) offers a non-invasive method for the local and dynamic characterisation of certain properties and structures of a sample. The aim of this work was to demonstrate the feasibility of using MRI *in situ* during the cooking of meat, and in particular imaging of the connective tissue to monitor deformation in the range 20-75 °C. The associated moisture loss was also estimated. Simulations of the temperature time course during cooking were carried out to relate deformation to sample temperature. The results showed that shrinkage began at 42 °C and accelerated from 54 °C. Migration of water from inside the fibres towards the interfascicular space appeared from 40°C and increased from 52 °C. These findings are consistent with those obtained by other, destructive and (or) non-localised methods. They will be used to determine deformation fields.

UR370 Qualité des Produits Animaux, INRA, F-63122 Saint Genès Champanelle.  
Phone: +33-4- 73-62-41-58. Fax: +33-4-73-62-40-89  
E-mail: mustapha.bouhrara@clermont.inra.fr

**Key words:** MRI, heating, deformation, moisture loss.

## I. INTRODUCTION

Knowledge of the structural changes that take place during treatment such as cooking is essential to enable meat industries to control the sensorial, nutritional and technical qualities of meat products. The cooking of meat causes a loss of approximately 20-40% of its mass, due to the expulsion of fluid (water and micronutrients) from the meat [1]. For the consumer, this moisture loss adversely affects quality, both sensorial (loss of tenderness and juiciness) and nutritional.

Several biophysical methods can be used to characterise the structure of meat [2]. During cooking, they can be used in particular to monitor the denaturing and precipitation of myosin [1, 3, 4, 5], the denaturing and shrinking of collagen [6] and the denaturing of other sarcoplasmic and myofibrillar proteins [7]. The mechanisms governing moisture loss have mainly been studied in raw meat [8, 9, 10], and less frequently in meat being heated [11, 12, 13].

The multi-exponential analysis of  $T_2$  relaxation curves of water obtained by low-field nuclear magnetic resonance (NMR) showed a water loss in the main population [14]. Amplitude variations in the most mobile population were also observed, but were more difficult to interpret without information on the localisation of that population. The only imaging study [11] conducted during meat cooking found that this moisture loss was associated with a decrease in water mobility during cooking. The spatial information only demonstrated differences between the core and the exterior of the sample, without giving any insight into the deformation or the mobility of the different water compartments

Our aim was to use MRI to study the impact of temperature on the deformation of the connective tissue and the resulting water transfer. MRI is a non-invasive imaging method, and so is well-suited to continuous monitoring during heating. In addition, susceptibility-weighted MRI shows the connective tissue of the meat [15, 16] which can provide an array of internal markers. The acquisition of a series of images during heating, and their *a posteriori* analysis, allows deformation fields to be determined. Lastly, the statistical parametric mapping of  $^1\text{H}$  nuclei allows water content and mobility to be locally quantified. This approach requires further methodological development (i) to acquire images at a fast enough rate to closely follow the changes in the meat during the heat treatment, and (ii) to ensure the feasibility of measurement in an evolving system.

The aim of the work described here was to demonstrate the feasibility of MRI during cooking, in particular imaging of the connective tissue. The acquisition of several images during the heat process allowed the deformation of the connective tissue to be followed in the temperature range 20-75 °C. Simulations of the meat temperature time course during cooking related the sample temperature, the deformation of the connective tissue and the resulting water transfer.

## II. MATERIALS AND METHODS

### A- Sample

The muscle sample used was the elastin-rich *biceps femoris (BF)* of a Charolais heifer (age 4 years). Before use it was matured for 7 days, then vacuum-packed and stored at  $-20^\circ\text{C}$ . It was thawed in air at  $20^\circ\text{C}$  and a cylinder of diameter 5 cm and length 6 cm long was cut from it with the

muscle fibres parallel to the cylinder axis. This cylinder was then again vacuum-packed to prevent direct contact with the circulating heating water.

### B- Description of the heating device

The sample holder (4, Fig.1) was fitted inside a heat-insulating Teflon® tube (5, Fig.1). This was in turn placed at the centre of the radiofrequency transmitter/receiver coil (6, Fig.1) itself placed inside the imager (7, Fig.1).

The sample was heated in its holder by water flowing in a circuit (3, Fig.1) fed by a pump (13 l/min) (2, Fig.1). The water was heated in a holding tank (1, Fig.1) by a temperature-regulated electric heating element. Heating by a liquid is preferable to heating by a gas because the heat exchange is more even. Among the possible liquids (which include oils) water was chosen for its simplicity in use, in particular when cleaning and draining the circuit.

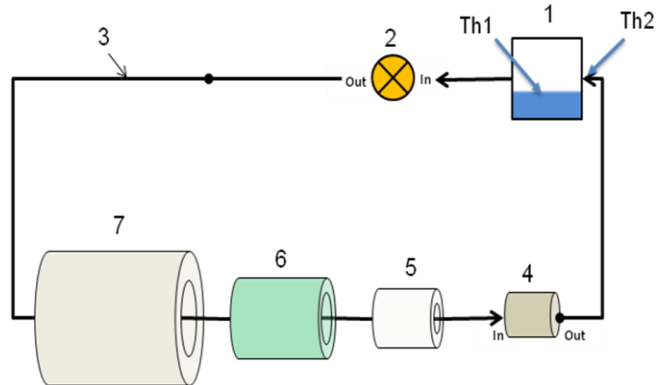


Fig.1. Diagram of set-up. (1) Holding tank and heating element for circulating water. (2) Pump. (3) 10 mm diameter silicone tubing. (4) Non-magnetic sample holder. (5) Non-magnetic Teflon® heat insulation. (6)  $^1\text{H}$  NMR antenna. (7) High-field NMR imager.

The adiabaticity of the heating system was checked by placing two thermocouples (Th1 and Th2) at each end of the circuit (tank Th1 and return flow Th2). The temperature was the same at the two measurement points, with a constant temperature rise of  $0.88\text{ }^\circ\text{C}/\text{min}$ .

### C- High-field MRI

Image acquisition was performed using a Biospec horizontal 4.7 tesla MRI system (Bruker GmbH, Ettlingen, Germany), of diameter 26 cm, fitted with a BGA-26 rapid gradient system (maximum amplitude  $50\text{ mTm}^{-1}$ , rise time  $260\text{ }\mu\text{s}$ ). The principal axis of the muscle fibres in the sample was parallel to the principal direction of the static magnetic field  $B_0$ .

The images were acquired continuously through a steady-state free precession sequence (SSFP or FLASH) that was weighted for magnetic susceptibility ( $T_E = 15\text{ ms}$ ,  $T_R = 2000\text{ ms}$ ). Using the difference in magnetic susceptibility between elastin and muscle fibres [15, 16], the images show the elastin-rich connective tissue (hyposignal). This sequence had bipolar gradients (delay between the two gradients  $\Delta = 5.52\text{ ms}$ , duration of each gradient  $\delta = 5.2\text{ ms}$ ) which

anceled out the signal from the mobile protons of the heating water. The removal of this signal eliminated the artefacts of movement, which degrade the image, and allows reducing the field of view (FOV), thereby increasing the temporal resolution for a given spatial resolution.

One acquisition consisted of a series of 18 contiguous radial sections. All the sections were obtained with a FOV of  $64 \times 64\text{ mm}^2$ , a matrix of  $256 \times 256$  pixels and a thickness of  $2\text{ mm}$ . The volume of the resulting voxel was  $0.5 \times 0.5 \times 2\text{ mm}^3$ . The temporal resolution was  $4\text{ min } 16\text{ s}$ . An acquisition was carried out at each temperature stage (every  $10\text{ }^\circ\text{C}$ ) and during each temperature rise between successive stages.

### D- Simulation of temperature

The temperature kinetics in the meat during cooking were calculated with a simple heat transfer model using the Comsol Multiphysics 3.4 software (COMSOL AB, Sweden 2007). Preliminary three-dimensional simulations showed that exchanges at the ends of the meat cylinder in contact with the polycarbonate support did not influence the temperature values in the central section of the cylinder.

Two-dimensional simulations by conduction were therefore carried out stepwise in this section; each step corresponded to a shrinkage of less than 5% of the surface bounded by the interface between the muscle and the exsuded water from MRI images. Between two steps the simulated temperature field was projected onto the new contracted meat surface, the rest of the domain being occupied by the volume of water exsuded.

The exchanges by water convection at the plastic bag surface were described by Newton's law, the heat transfer coefficient being calculated from the velocity of the circulating fluid and the Churchill-Bernstein relation [17]. The thermophysical properties of the products (plastic bag, meat, exsudate) were those used classically in the literature. Simplifying hypotheses were applied: (i) the volume of the plastic bag was assumed to be constant, and the volume of the exsudate formed during cooking was assumed to be equal to the decrease in volume of the contracted meat, and (ii) the heat transfer in the bag was assumed to be purely conductive. The temperature at the surface of the plastic bag was that measured experimentally in the circulating water.

## III. RESULTS AND DISCUSSION

### A- Feasibility of connective tissue imaging

The resonance frequency of the antenna/sample set and the impedance of the resonating cavity at this frequency changed with the temperature. These two drifts caused a signal loss of  $\sim 10\%$  between  $20\text{ }^\circ\text{C}$  and  $75\text{ }^\circ\text{C}$ . The additional signal loss of  $\sim 40\%$  observed between the two images obtained at  $20\text{ }^\circ\text{C}$  and  $75\text{ }^\circ\text{C}$  (Fig.2) was essentially due to the changes in the intrinsic NMR parameters of the muscle, in particular  $T_2$  and

the proton density, which decreased respectively by 25% and 30%.

The signal loss due to resonant cavity drift was minor compared with the losses due to changes in the sample. It was therefore not strictly necessary to adjust the antenna/sample settings manually. Also, the signal loss observed was tolerable as the final temperature (75 °C) displayed an acceptable signal-to-noise ratio (SNR ~ 21).

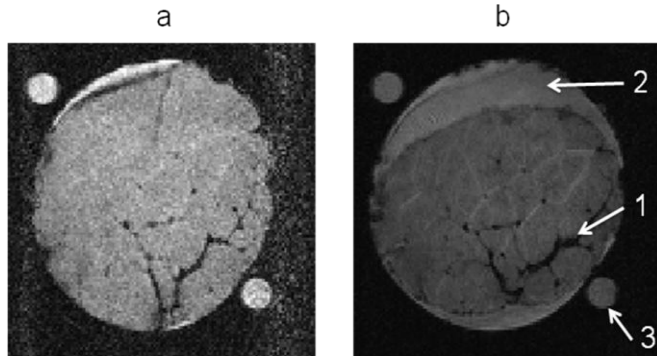


Fig.2. Susceptibility-weighted MRI images of a core section for the same grey scale (a) at 20 °C, (b) at 75 °C. 1: connective tissue, 2: fluid exsuded from muscle, 3: reference tube.

### B- Monitoring of connective tissue deformations

Fig.3 shows deformation images obtained at the core of the sample as a function of the heating water temperature (Fig.3.a), and images of corresponding temperature gradients obtained by simulation (Fig.3.b). The plots (Fig.3.c) represent the time course of the surface of the core section of the muscle calculated from NMR images, the evolution of the temperature of heating water and the evolution of the mean temperature of the muscle obtained by simulation using shape information provided by NMR images.

Fig.3.a shows four representative images out of a series of 18 images recorded at different temperatures. The deformation time course plot (Fig.3.c) shows two inflection points, the first at 73 min, corresponding to the start of the sample deformation at the mean muscle temperature of 42 °C (heating water temperature 50 °C), and the second at 96 min, highlighting an acceleration of the deformation at a mean muscle temperature of 55 °C (heating water temperature 62 °C). Between 20 °C and 75 °C, the surface area of the muscle core section decreased by 22%.

The deformation images (Fig.3.a) reveal a network of exsuded water channels among the fibre bundles resulting from migration of intracellular water [10, 20]. This water was characterised by a higher  $T_2$  value (more mobile water), which gave a hypersignal on the weighted image  $T_2^*$ . This effect was seen from the mean muscle temperature of 40 °C (heating water temperature 47 °C). Like the connective tissue, these channels can serve as internal markers to determine deformation fields.

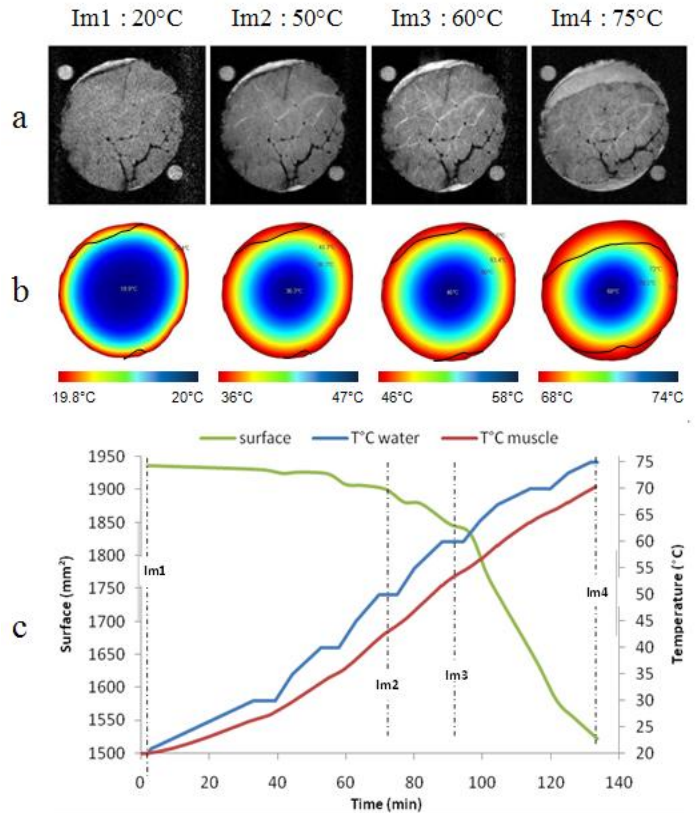


Fig.3. (a) NMR deformation images of a core section at different temperatures of the heating water, (b) images simulating corresponding temperature gradients, (c) time course plots of the surface area of the muscle core section, the temperature of the heating water and the mean muscle temperature.

The results of this study are consistent with those reported in the literature, in particular: (i) start of the deformation observed at 42 °C, corresponding to the beginning of myosin denaturation [1, 3, 4, 5] with a slow transverse contraction of the myofibres [18], and (ii) acceleration of deformation at 55 °C, corresponding to shrinkage and denaturation of collagen with expulsion of meat juice [1, 6, 7, 19].

The appearance of channels of migrating water among the fibre bundles (Fig.3.a) began from 40 °C. The initial denaturation of myosin causes a small loss of water from myofibres. This water migrates into the inter-myofibre space [10, 20]. The effect was more obvious from 52 °C, probably due to the contraction of the connective tissue, which expels water first into the interfascicular space and then out of the meat.

## IV. CONCLUSION

This work demonstrates the feasibility of connective tissue imaging during cooking using an MRI-compatible heating system with high adiabaticity. This imaging allowed, for the first time, the monitoring of meat deformation during cooking between 20 °C and 75 °C. Our observations are consistent

with literature data for the temperatures of structural protein denaturation, collagen contraction and water loss.

Future work is planned to improve the temporal resolution of the method using rapid image encoding (e.g. echo planar imaging), determine deformation fields and quantify local water content.

#### ACKNOWLEDGEMENTS

This work was funded by the EU project ProSafeBeef ([www.prosafebeef.eu/asp/](http://www.prosafebeef.eu/asp/)).

#### REFERENCES

- [1] Bertram, H. C., Engelsen, S. B., Busk, H., Karlsson, A. H., & Andersen, H. J. (2004). Water properties during cooking of pork studied by low field NMR relaxation: effects of curing and the RN-gene. *Meat Science*, 66, 437–446.
- [2] Damez, J. L., & Clerjon, S. (2008). Meat quality assessment using biophysical methods related to meat structure. *Meat Science* 80, 132–149.
- [3] Martens, H., & Vold, E. (1976). DSC studies of muscle protein denaturation. In Proceedings of the 22nd European meeting of meat research workers, Malmö, Sweden (p. J 9.3).
- [4] Micklinder, E., Peshlov, B., Purslow, P. P., & Engelsen, S. B. (2002). NMR-cooking monitoring the changes in meat during cooking by low-field H-NMR. *Trends in Food Science & Technology*, 13, 341–346.
- [5] Martens, H., Stabursvik, E., & Martens, M. (1978). Texture and colour changes in meat during cooking related to thermal denaturation of muscle proteins. *Journal of Texture Studies*, 13, 291–309.
- [6] Stabursvik, E., & Martens, H. (1980). Thermal denaturation of proteins in post rigor muscle tissue as studied by differential scanning calorimetry. *Journal of Science Food and Agriculture*, 31, 1034–1042.
- [7] Wright, D. J., Leach, I. B., & Wilding, P. (1977). Differential scanning calorimetric studies of muscle and its constituents. *Journal of Science Food and Agriculture*, 28, 557.
- [8] Bertram, H. C., Dønstrup, S., Karlsson, A. H., & Andersen, H. J. (2002). Continuous distribution analysis of T2 relaxation in meat: an approach in the determination of water-holding capacity. *Meat Science*, 60, 279–285.
- [9] Renou, J. P., Foucat, L., & Bonny, J. M. (2003). Magnetic resonance imaging studies of water interactions in meat. *Food Chemistry*, 82, 35–39.
- [10] Bertram, H. C., Whittaker, A. K., Andersen, A. J., & Karlsson, A. H. (2004). Visualization of drip channels in meat using NMR microimaging. *Meat Science*, 68, 667–670.
- [11] Shaarani, S. Md., Nott, K. P., & Hall, L. D. (2006). Combination of NMR and MRI quantitation of moisture and structure changes for convection cooking of fresh chicken meat. *Meat Science*, 72, 398–403.
- [12] Wählby, U., Skjöldebrand, C. (2001). NIR-measurements of moisture changes in foods. *Journal of Food Engineering*, 47, 303–312.
- [13] Van der Sman, R.G.M. (2007). Moisture transport during cooking of meat: An analysis based on Flory–Rehner theory. *Meat Science*, 76, 730–738.
- [14] Tornberg, E. (2005). Effects of heat on meat proteins: Implications on structure and quality of meat products. *Meat Science*, 70, 493–508.
- [15] Bonny, J. M., Laurent, W., Labas, R., Taylor, R., Berge, P., & Renou, J. P. (2001). Magnetic resonance imaging of connective tissue: a non-destructive method for characterizing muscle structure. *Journal of the Science of Food and Agriculture*, 81, 337–341.
- [16] Bonny, J. M. (2007). Magnetic resonance imaging of meat: Towards the non-destructive determination of extracellular matrix composition and distribution. *GIT laboratory Journal*, 11, 30–31.
- [17] Churchill, S.W., & Bernstein, M. (1977). A Correlating Equation for Forced Convection from Gases and Liquids to a Circular Cylinder in Cross Flow. *J. Heat Transfer*, 99, 300–306.
- [18] Bendall, J. R., & Restall, D. J. (1983). The cooking of single myofibres, small myofibre bundles and muscle strips from beef *M. Psoas* and *M. Sternomandibularis* muscles at varying heating rates and temperatures. *Meat Science*, 8, 93–117.
- [19] Palka, K., & Daun, H. (1999). Changes in texture, cooking losses, and myofibrillar structure of bovine M-semitendinosus during heating. *Meat Science*, 51, 237–243.
- [20] Bonny, J.M., & Renou, J.P. (2002). Water diffusion features as indicators of muscle structure ex vivo. *Magnetic Resonance Imaging* 20, 395–400.